Swansea University
Prifysgol Abertawe

Cronfa
Setting Research Free

Cronfa - Swansea University Open Access Repository

_____

This is an author produced version of a paper published in:
8th GACM Colloquium on Computational Mechanics for Young Scientists from Academia and Industry, 2019

Cronfa URL for this paper:
http://cronfa.swan.ac.uk/Record/cronfa52125

_____

Conference contribution :

Hossain, M. & Liao, Z. (2019).   *Towards thermo-viscoelastic experimental characterisation and numerical modelling of VHB polymer.* 8th GACM Colloquium on Computational Mechanics for Young Scientists from Academia and Industry, 2019, Kassel, Germany: German Association of Computational Mechanics.
http://dx.doi.org/10.19211/KUP9783737650939

_____

Towards thermo-viscoelastic experimental characterisation and numerical modelling of VHB polymer

Mokarram Hossain[*][1] and Zisheng Liao[2]

[1] Zienkiewicz Centre for Computational Engineering, Swansea University, UK
[2] School of Civil Engineering and Transportation, South China University of Technology, China

Abstract. In this study, we have presented a wide variety of temperature experiments of a commercially available VHB polymer ranging from -30°C to 80°C at various strain rates and stretch levels under homogeneous deformation and temperature fields. The study demonstrates a pronounced influence of the temperature field on mechanical responses of the VHB polymer. After a wide range of experiments, we have proposed a finite-strain thermo-viscoelastic constitutive model where a non-linear evolution law is devised based on the classical concept of multiplicative decomposition of the deformation gradient. Then, decoupled one-dimensional equations are fitted to identify relevant material parameters appearing in the model. The thermo-viscoelastic model validation shows its excellent capability to predict the experimental results.

1 Introduction

The so-called Very High Bond (VHB in short) becomes an ideal polymer for producing prototypes of electric field-responsive functional materials, e.g., actuators in soft robotics, stretch sensors in wearable devices, and energy harvesters from ambient motions. The commercially available polymer comes up with several thicknesses. For this study, we have selected VHB 4905 thanks to its wide use as a common material for dielectric elastomers. The acrylic-based polymer is highly deformable, extremely viscoelastic, and highly sensitive to temperature fluctuations. Hence, in order to understand its mechanical and electro-mechanical behaviours, extensive experiments need to be conducted to demonstrate temperature dependencies in addition to rate-dependences. The aims of the current work are twofolds. On the one hand, a complete thermo-viscoelastic mechanical characterization of VHB 4905 is presented considering some standard experiments suitable for viscoelastic polymers at large strains, e.g. loading-unloading cyclic tests, quasi-static tests at very slow strain rates, single-step relaxation tests, and multi-step relaxation tests under homogeneous thermo-mechanical loads. On the other hand, a thermodynamically consistent phenomenologically-motivated geometrically non-linear thermo-viscoelastic material model is developed for VHB polymers. At this stage, all experiments are performed under a homogeneous deformation, both mechanical and thermal loads. Hence, the three-dimensional thermo-viscoelastic model is decoupled to a set of one-dimensional equations. After that, all relevant parameters appearing in the model are identified by a simultaneous optimisation routine. Once all necessary material parameters are identified, the model fits well with the data that are not included during the identification process, see [1, 2].

2 Experimental study

In order to characterize viscoelastic behaviours of the VHB polymer, at first cyclic experiments are carried out with regard to different deformations, strain rates, and temperatures. In these experiments, we adopt three different deformation levels, i.e., 100%, 200%, and 300%, three different strain rates, i.e., 0.1 /s, 0.05 /s and 0.03 /s, and eight different temperature profiles, i.e. 80°C, 60°C, 40°C, 20°C, 0°C, -20°C, -30°C and -40°C. Results are presented in Figs 1 and 2. In Fig 1, temperature-dependent results are presented ranging from -20°C to + 60°C temperatures while experiments are conducted at a strain rate of 0.1/s with deformations of 300%. These graphs indicate that at all tested temperatures, a larger deformation

---

[*]**Corresponding author:** mokarram.hossain@swansea.ac.uk **ORCID iD:** ORCID:https://orcid.org/0000-0002-4616-1104
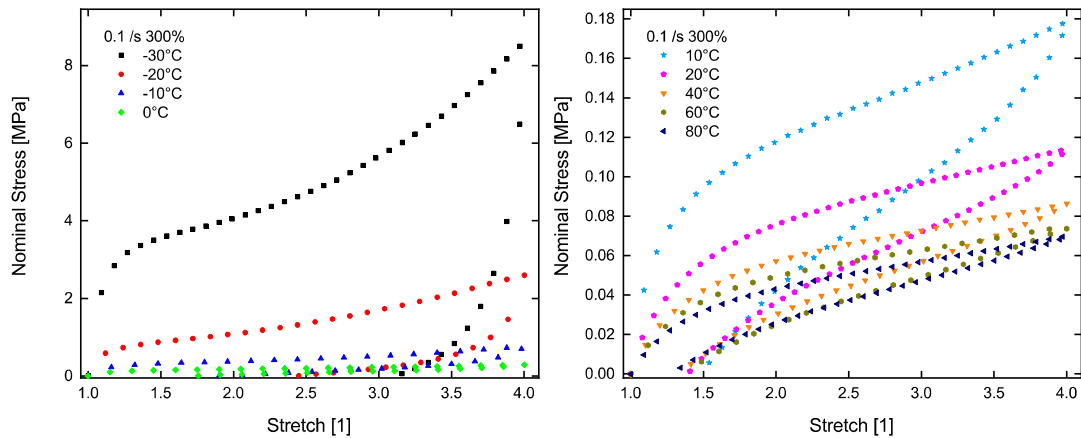
Figure 1. Temperature-dependent stress responses under a wide range of temperature profile where experiments are conducted at 300% deformation and 0.1 /s strain rate, (Left) below 0°C, (Right) above 0°C. All results clearly reveal that the temperature field has a major role in changing mechanical stress responses of VHB
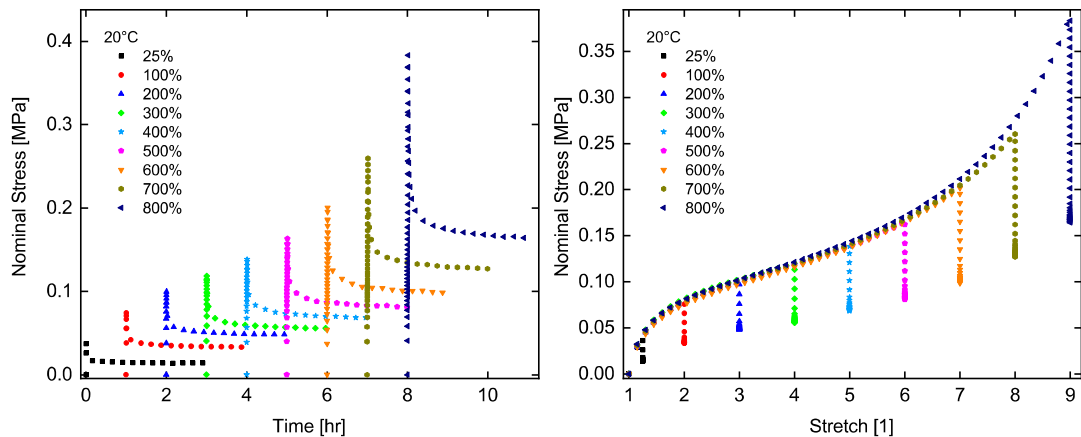

Figure 2. (Left) Single step relaxation test results from 25% to 800% deformations. (Right) Stress-strain curves of multi-step tests depicting the amount of stress relaxations during the holding times

results in a bigger hysteresis with a larger residual strain. Moreover, it is clear that the nonlinearity of the stress-stretch response is getting stronger from a higher to a lower temperature at the same strain. These results also demonstrate that the VHB 4905 becomes less dissipative with an increasing positive temperature.

Single-step relaxation experiments are performed on tensile specimens from 100% to 800% deformations with an internal of 100% deformations. For a better demonstration purpose, the stress history curves are shifted along the time axis to avoid overlapping of the curves, as is shown in Fig 2(left). From the results, it can be observed that with the time evolving, the stress attenuates to an equilibrium level. However, at a larger strain, it takes a longer time to relax. This implies that at a larger deformation level, more relaxation time is required to obtain an equilibrium stress. Another way to identify the equilibrium stress of a polymeric material is the multi-step relaxation tests. Similar to the single step relaxation experiments, the specimen is stretched to a certain strain level and is allowed to relax for a three-hour period before the specimen is re-loaded to the next strain level instead of being unloaded. In this case, a multi-step relaxation experiment is carried out at an interval of 100%, 300%, 500% , and 700%. As is shown in Fig 2(right) the single step relaxation tests and the corresponding steps of the multi-step relaxation tests share similar relaxation history curves with very close relaxed stresses (equilibrium stresses).

3 Numerical modelling

In uniaxial tests, the specimen is elongated only in one direction, i.e., $\lambda_1 = \lambda$ while the other two directions are free to move. From the incompressibility condition at fixed temperature, i.e., $\det \boldsymbol{F} = \det \bar{\boldsymbol{F}} = \det \boldsymbol{F}_v = \det \boldsymbol{F}_\Theta = 1$, i.e., $\lambda_1 \lambda_2 \lambda_3 = 1$ and the assumption of symmetry the complementary principal stretches follow as $\lambda_2 = \lambda_3 = \lambda^{-1/2}$. Therefore, the complete deformation gradient reads $\boldsymbol{F} = \{\lambda; \lambda^{-1/2}; \lambda^{-1/2}\}$. Note that since the elongation is only in one direction, the specimen will contract in the transversal directions and due to the stress-free boundary conditions, both Piola stresses P_2 and P_3 are zero and only the Piola stress P_1 needs to be determined. The elastic part of the Piola stress is obtained:

$$P^e = \left[\frac{\Theta}{\Theta_0} + g^e(\Theta)\right]\left[2a + 8b[2\lambda^{-1} + \lambda^2]^3 + c[1 + 2\lambda^3]^{-\frac{1}{2}}\right]\left[\lambda - \lambda^{-2}\right] \tag{1}$$

for details, see [1, 3, 4]. Note that since we have observed negligible influence of the temperature on the equilibrium response during our study, $g^e(\Theta) = 1 - \frac{\Theta}{\Theta_0}$ is taken here. Now, the viscous part of the stress for a single Maxwell element is formulated :

$$
\begin{aligned}
P^v &= \left[\frac{\Theta}{\Theta_0} + g_1^v(\Theta)\right]\sum_{j=1}^{2} P^{v,j} + \left[\frac{\Theta}{\Theta_0} + g_2^v(\Theta)\right]\sum_{j=3}^{5} P^{v,j} \\
&= \left[\frac{\Theta}{\Theta_0} + g_1^v(\Theta)\right]\sum_{j=1}^{2} 6c_4^j \left[\frac{\lambda^2}{[\lambda_v^j]^2} + \frac{2\lambda_v^j}{\lambda} - 3\right]^2 \left[\frac{\lambda}{[\lambda_v^j]^2} - \frac{\lambda_v^j}{\lambda^2}\right] \\
&\quad + \left[\frac{\Theta}{\Theta_0} + g_2^v(\Theta)\right]\sum_{j=3}^{5} 2c_5^j \left[\frac{\lambda}{[\lambda_v^j]^2} - \frac{\lambda_v^j}{\lambda^2}\right],
\end{aligned} \tag{2}
$$

where λ_v^2 is the principal stretch of the internal variable. Similar to the one-dimensional formulation of the total stress, the first evolution law is derived:

$$\dot{\lambda_v^j} = \frac{4}{\tau_1^j}\left[\frac{\lambda^2}{[\lambda_v^j]^2} + \frac{2\lambda_v^j}{\lambda} - 3\right]^2 \left[\frac{\lambda^2}{\lambda_v^j} - \frac{[\lambda_v^j]^2}{\lambda}\right], \qquad j = 1, 2 \tag{3}$$

and the one-dimensional form of the second evolution equation is

$$\dot{\lambda_v^j} = \frac{4}{3\tau_2^j}\left[\frac{\lambda^2}{\lambda_v^j} - \frac{[\lambda_v^j]^2}{\lambda}\right], \qquad j = 3 \cdots 5. \tag{4}$$

Now both the scalar-valued differential equations need to be discretized by a suitable integration scheme. Discretizing by the unconditionally stable implicit Euler-backward integration scheme, the differential equation for the internal variable λ_v^j for a single Maxwell element yields

$$
\begin{aligned}
\lambda_v^j &= \lambda_v^{j,n} + \frac{4\Delta t}{3\tau_2^j}\left[\frac{\lambda^2}{\lambda_v^j} - \frac{[\lambda_v^j]^2}{\lambda}\right], \\
f(\lambda_v^j) &= \lambda_v^j - \lambda_v^{n,j} - \frac{4\Delta t}{3\tau_2^j}\left[\frac{\lambda^2}{\lambda_v^j} - \frac{[\lambda_v^j]^2}{\lambda}\right]
\end{aligned} \tag{5}
$$

where $[\bullet]^k = [\bullet](t_k)$ and $\Delta t = t_{n+1} - t_n$. For the sake of brevity, the index for the current value (t_{n+1}) of the stretch λ_v^j has been dropped in Eqn (5). Eqn (5) is non-linear in terms of λ_v^j. Therefore, a Newton-type iterative scheme is required to find the current value of λ_v^j that need to be inserted in Eqn (2) to obtain the updated value of the total Piola stress, $P(t) = P^e + P^v(t)$.

4 Model validation

For the identification of hyperelastic material parameters appearing in a model, three main procedures have been discussed in the literature, see [2]. The first option is to perform single-step relaxation experiments at various strain levels. When a test specimen is held at a certain strain, the stress will gradually
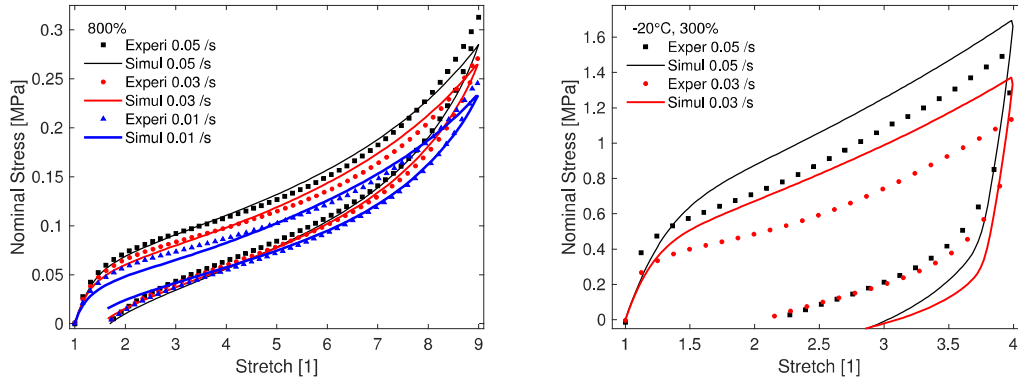
Figure 3. Viscoelastic parameter identification: Three different strain rates are used to identify viscous parameters while hyperelastic parameters identified earlier are kept frozen. Total five Maxwell elements, each having two material parameters, are well enough to capture the strain rate-dependent data up to 800% deformations. (Right) Model performance is validated by other strain rate dependent tests

reduce and will asymptotically reach an equilibrium stress state, which can be considered as the relaxed and basic elastic stress at the corresponding strain. The next step is to identify the viscoelastic parameters. With the hyperelastic parameter, the equilibrium stress can be calculated, and the over-stress modulus and over-stress relaxation spectrum are yet to be identified in order to obtain the viscous over-stress. Since viscoelasticity is the strain rate dependent behavior, we identify the parameters using three sets of data at 800% strain and at different strain rates, which are 0.01 /s, 0.03 /s, and 0.05 /s, simultaneously. Note that during the identification process, we find that five sets of Maxwell elements can capture the viscoelastic behavior with a fair accuracy while more elements could not improve the results significantly, cf Fig 3 (left). During the viscoelastic parameter identification, hyperelastic parameters are kept fixed. With the identified parameters, both strain rate dependences and large strain nonlinearities are captured successfully, see Fig 3(right).

5 Conclusion

In this contribution, a detail thermo-viscoelastic experimental characterizations of a widely-used VHB polymer is presented. All experiments were performed in a purposively-built temperature chamber that can operate under a wide span of temperature ranging from -50°to 150°C. In order to quantify viscoelastic behaviours of the polymer, all classical experimentations, i.e., quasi-static tests at very low strain rates, single-step and multi-step relaxation tests, loading-unloading cyclic tests were conducted at different strain rates and at different temperature profiles. Exploring the experimental data obtained in the current study, a thermodynamically consistent phenomenologically motivated thermo-viscoelastic material model at finite strain is proposed. Once, a complete set of viscoelastic parameters are identified, we use them to validate other sets of data that are not utilised in any identification process. All validation examples show an excellent agreement between model and experimental data.

References

[1] Z. Liao, M. Hossain, X. Yao, M. Mehnert, P. Steinmann, *On thermo-viscoelastic experimental characterisations and numerical modelling of VHB polymer*, In Review, 2019

[2] M. Hossain, D. K. Vu, P. Steinmann, *Experimental study and numerical modelling of VHB 4910 polymer*, Computational Materials Science, 59:65-74, 2012

[3] P. Steinmann, M. Hossain and G. Possart, *Hyperelastic models for rubber-like materials: Consistent tangent operators and suitability of Treloar's data*, Arch. of Appl. Mech., 82(9):1183-1217, 2012

[4] M. Hossain, P. Steinmann, *More hyperelastic models for rubber-like materials: Consistent tangent operator and comparative study*, Journal of Mechanical Behaviour of Materials, 22(1-2):27-50, 2013